PHYSICAL REVIEW B **96**, 041104(R) (2017)

Strong correlation effects on surfaces of topological insulators via holography

Yunseok Seo, Geunho Song, and Sang-Jin Sin
Department of Physics, Hanyang University, Seoul 04763, Korea

(Received 23 March 2017; published 5 July 2017)

We investigate the effects of strong correlation on the surface state of a topological insulator (TI). We argue that electrons in the regime of crossover from weak antilocalization to weak localization are strongly correlated, and calculate the magnetotransport coefficients of TIs using the gauge-gravity principle. Then, we examine the magnetoconductivity (MC) formula and find excellent agreement with the data of chrome-doped Bi_2Te_3 in the crossover regime. We also find that the cusplike peak in MC at low doping is absent, which is natural since quasiparticles disappear due to the strong correlation.

DOI: 10.1103/PhysRevB.96.041104

Introduction. Understanding strongly correlated electron systems has been a theoretical challenge for several decades. Typically, such systems lose quasiparticles and show mysteriously rapid thermalization [1–4], which provides their hydrodynamic description [5,6] near the quantum critical point (QCP). Recently, the principle of gauge-gravity duality [7–9] has attracted much interest as a possible paradigm for strongly interacting systems, where the system near QCP is mapped to a black hole. More recently, a large violation of the Widermann-Frantz law was observed in graphene near the charge neutral point, indicating that it is a strongly interacting system [10] in a specific range of temperature, and the gauge-gravity principle applied to it exhibited remarkable agreement with the experimental data [11].

The fundamental reason for the appearance of a strong interaction in graphene is the *smallness of the Fermi sea*: In the presence of a Dirac cone, when the Fermi surface is near the tip of the cone, the electron-hole pair creation from such a small Fermi sea is insufficient to screen the Coulomb interaction. Because this is so simple and universal, one can expect that for any Dirac material, there should be a regime of parameters where electrons are strongly correlated. The Dirac cone also provides the reason why it is a quantum critical system with Lorentz invariance. The most well-known Dirac material other than graphene is the surface of a topological insulator (TI) [12,13]. The latter has an unpaired Dirac cone and strong spin-orbit coupling, and, as a consequence, it has a variety of interesting physics [14–16], including weak antilocalization (WAL) [17].

Magnetic doping in TIs can open a gap in the surface state by breaking the time reversal symmetry (TRS) [18–20], and it is responsible for the transition from WAL to weak localization (WL). For extremely low doping, the sharp horn of the magnetoconductivity curve near a zero magnetic field can be described by the Hikami-Larkin-Nagaoka (HLN) function [21]. However, for intermediate doping where the tendency for WAL and weak localization (WL) is to compete, a satisfactory theory is still lacking [18,20,22], although a phenomenological description exists [23]. Even in the case where the Fermi surface is large at low doping so that the system is a Fermi liquid, increasing the surface gap pushes up the dispersion curve, which makes the Fermi sea small. Then, the logic for strong coupling in graphene works for the transition region in the surface of a TI. Therefore, an electron system near the transition region should be strongly correlated.

In this Rapid Communication, we investigate magnetoconductivity (MC) for the surface of a topological insulator with correlated electrons using the gauge-gravity principle. We will give analytic formulas for all magnetotransport on the surface of TIs with strong correlations as a function of magnetic field, temperature, and impurity density, and compare the results with the Bi_2Te_3 data of Ref. [20]. Most interestingly, in the doping regime with a crossover from WAL to WL, our theory agrees nicely with the experimental data in a specific range of temperature, justifying our suggestion that electrons in the experimented material are strongly correlated in this regime. Our results also show that the cusplike peak in the MC curve at a fixed temperature, which is the hallmark of WAL in weakly interacting systems, is absent, which can be argued to be a consequence of strong correlation.

Idea of the model. Our system is the surface of a topological insulator which is a $(2+1)$-dimensional system with an odd number of Dirac cones. Our question is what happens if such a system has a strong correlation as well, and the recipe for strong electron-electron interactions is to use the gauge-gravity principle or holography. For TIs, special care is necessary to encode strong spin-orbit coupling (SOC). Our holographic model is defined on a manifold $\mathcal{M}$, which is asymptotically AdS_4. With this setup, our model is defined by the action

$$2\kappa^2 S = \int_{\mathcal{M}} d^4x\sqrt{-g}\left[R + \frac{6}{L^2} - \frac{1}{4}F^2 - \sum_{I,a=1,2}\frac{1}{2}\left(\partial\chi_I^{(a)}\right)^2\right] - \frac{q_\chi}{16}\int_{\mathcal{M}}\sum_{I=1,2}\left(\partial\chi_I^{(2)}\right)^2 F\wedge F, \tag{1}$$

where q_χ is the coupling, $\kappa^2 = 8\pi G$, and L is the AdS radius. From now on, we set $2\kappa^2 = L = 1$. The action contains two pairs of bosons, one for the magnetic impurities and the other for the nonmagnetic ones. To encode the effect of SOC in the presence of magnetic doping, we introduced the last term, which is a coupling between the impurity density and the instanton density. Such an interaction term was first introduced in Ref. [24] by us to discuss the SOC. A strong SOC provides the band inversion that induces massless chiral fermions at the boundary, which in turn induces the chiral anomaly as a nontrivial divergence of the chiral current. In fact, our interaction term is unique in that it is the leading order term that can take care of the anomaly and its coupling to the impurity in a manner with broken time reversal symmetry.

The solution of the equation of motion is given by

$$A = a(r)dt + \tfrac{1}{2}H(xdy - ydx),$$
$$\chi_I^{(1)} = \alpha\begin{pmatrix} x \\ y \end{pmatrix}, \quad \chi_I^{(2)} = \lambda\begin{pmatrix} x \\ y \end{pmatrix},$$
$$ds^2 = -U(r)dt^2 + \frac{dr^2}{U(r)} + r^2(dx^2 + dy^2), \tag{2}$$

with

$$U(r) = r^2 - \frac{\alpha^2 + \lambda^2}{2} - \frac{m_0}{r} + \frac{q^2 + H^2}{4r^2} + \frac{\lambda^4 H^2 q_\chi^2}{20r^6} - \frac{\lambda^2 H q q_\chi}{6r^4},$$
$$a(r) = \mu - \frac{q}{r} + \frac{\lambda^2 H q_\chi}{3r^3}, \tag{3}$$

where μ is the chemical potential, and q is the charge carrier density. q and m_0 are determined by the regularity condition at the black hole horizon, $A_t(r_0) = U(r_0) = 0$,

$$q = \mu r_0 + \tfrac{1}{3}\theta H \quad \text{with} \quad \theta = \frac{\lambda^2 q_\chi}{r_0^2}, \tag{4}$$
$$m_0 = r_0^3\left(1 + \frac{r_0^2\mu^2 + H^2}{4r_0^4} - \frac{\alpha^2 + \lambda^2}{2r_0^2}\right) + \frac{\theta^2 H^2}{45 r_0}. \tag{5}$$

Usually the chemical potential is proportional to the charge density. However, in our model, there is an extra term $\sim\theta H$, which represents the Witten effect, the magnetic field generation by electric charge and vice versa. It comes from the last term of the action whose microscopic origin is the spin-orbit interaction [25,26].

The temperature of the physical system is identified by the Hawking temperature of the black hole given by

$$T = \frac{12r_0^4 - \left[H^2 + 2r_0^2(\alpha^2 + \lambda^2) + (q - H\theta)^2\right]}{16\pi r_0^3}, \tag{6}$$

and the entropy and energy densities are given by $s = 4\pi r_0^2$ and $\epsilon = 2m_0$, respectively. Since the boundary on-shell action is related with pressure by $S_{\text{on-shell}} = -\mathcal{P}$, we get $\varepsilon + \mathcal{P} = sT + \mu q$. Then, the magnetization can be obtained from $M = -\frac{\partial\epsilon}{\partial H}$.

The *dc transport coefficients* can be calculated by turning on small fluctuations around the background (3) [27],

$$\delta G_{ti} = -tU(r)\zeta_i + \delta g_{ti}(r), \quad \delta G_{ri} = r^2\delta g_{ri},$$
$$\delta A_i = t[-E_i + \zeta_i a(r)] + \delta a_i(r), \tag{7}$$

where $i = x,y$. Notice that the equations of motion for fluctuation are time independent, although there is an explicit time dependence above the ansatz. Here, E_i corresponds to the external electric field and $\zeta_i = -\partial_i T/T$. We define the bulk currents by

$$\mathcal{J}^i = \sqrt{-g}F^{ir}, \quad \mathcal{Q}^i = U(r)^2\partial_r\left(\frac{\delta g_{ti}(r)}{U(r)}\right) - a_t(r)J^i, \tag{8}$$

which become the electric and the heat current J^i and $Q^i = \langle T^{ti}\rangle - \mu J^i$, respectively, at the boundary ($r \to \infty$). Using the equations of motion of the fluctuation fields together with the horizon regularity condition, we can get the electric and heat current at the boundary in terms of the external sources,

$$J^i = \frac{(\mathcal{F} + \mathcal{G}^2)(\mathcal{F} - H^2)}{\mathcal{F}^2 + H^2\mathcal{G}^2}E_i + \left[\theta + \frac{H\mathcal{G}(2\mathcal{F} + \mathcal{G}^2 - H^2)}{\mathcal{F}^2 + H^2\mathcal{G}^2}\right]\epsilon_{ij}E_j + \frac{sT\mathcal{G}(\mathcal{F} - H^2)}{\mathcal{F}^2 + H^2\mathcal{G}^2}\zeta_i + \frac{sTH(\mathcal{F} + \mathcal{G}^2)}{\mathcal{F}^2 + H^2\mathcal{G}^2}\epsilon_{ij}\zeta_j,$$
$$Q^i = \frac{sT\mathcal{G}(\mathcal{F} - H^2)}{\mathcal{F}^2 + H^2\mathcal{G}^2}E_i + \frac{sTH(\mathcal{F} + \mathcal{G}^2)}{\mathcal{F}^2 + H^2\mathcal{G}^2}\epsilon_{ij}E_j + \frac{s^2T^2\mathcal{F}}{\mathcal{F}^2 + H^2\mathcal{G}^2}\zeta_i + \frac{s^2T^2H\mathcal{G}}{\mathcal{F}^2 + H^2\mathcal{G}^2}\epsilon_{ij}\zeta_j, \tag{9}$$

where $\zeta_i = -(\nabla_i T)/T$ as before and

$$\mathcal{F} = r_0^2(\alpha^2 + \lambda^2) + (1 + \theta^2)H^2 - q\theta H,$$
$$\mathcal{G} = q - \theta H. \tag{10}$$

Now, the transport coefficients can be read off from

$$\begin{pmatrix} J^i \\ Q^i \end{pmatrix} = \begin{pmatrix} \sigma_{ij} & \alpha_{ij}T \\ \bar{\alpha}_{ij}T & \bar{\kappa}_{ij}T \end{pmatrix}\begin{pmatrix} E_j \\ \zeta_j \end{pmatrix}. \tag{11}$$

In the $q_\chi \to 0$ limit, Eqs. (9) are reduced to those of the dyonic black hole [28–31]. There are two important symmetries of the dc conductivities: One is the antisymmetry of the off-diagonal components, i.e., $X_{ij} = -X_{ji}$ for all $X = \sigma,\alpha,\bar{\kappa}$, and the other is $\alpha_{ij} = \bar{\alpha}_{ij}$, which is Onsager's relation. If we further take the $H \to 0$ limit,

$$\sigma_{xx} \to 1 + \frac{q^2}{r_0^2(\alpha^2 + \lambda^2)}. \tag{12}$$

Notice that if we define $\beta^2 = \alpha^2 + \lambda^2$, $\gamma = \frac{\lambda^2}{\alpha^2 + \lambda^2}$, then β^2 plays the role of the total impurity density used in Ref. [24], and λ^2 and α^2 can be interpreted as the magnetic and nonmagnetic impurity density, respectively. Therefore, γ corresponds to the magnetic doping parameter, which is usually denoted by x in the literature.

Magnetoconductance. To compare our results with the data for the nonferromagnetic material, we take $\mu = 0$ to set the ferromagnetic magnetization zero. The longitudinal conductivity in this limit is

$$\sigma_{xx} = \frac{(\mathcal{F} + \mathcal{G}^2)(\mathcal{F} - H^2)}{\mathcal{F}^2 + H^2\mathcal{G}^2}. \tag{13}$$

The MC is defined by $\Delta\sigma \equiv \sigma_{xx}(H) - \sigma_{xx}(0)$.

Consider the evolution of the system with doping. As the surface gap increases, the size of the Fermi surface decreases. See Fig. 1(a). At $x = 0.08$, the gap is large enough to see a transition from WAL to WL for some temperatures, but the Fermi surface is still large so that the particle character remains. At $x = 0.1$, the gap is large enough and the Fermi surface is small enough to show strong coupling behavior, so that our theory

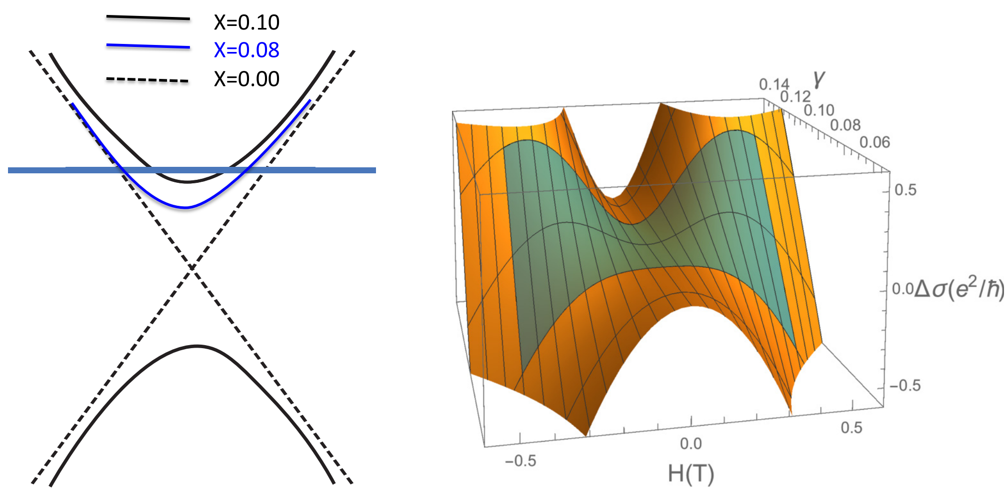

(a) (b)

FIG. 1. Evolution of (a) density of states and (b) MC as we vary the doping. Again, our theory fits the data only in an island of parameter space (H,γ), where $\gamma = x$. We took care of the factor 2 for the spin degeneracy in MC.

is well applicable. Figure 1(b) shows the evolution of the MC curve as we increase the doping rate, assuming that the entire regime can be described holographically. However, the real system is strongly correlated only when the Fermi surface is small enough. Therefore, we expect that our theory is valid only in a specific window of the doping rate as well as that of temperature. This is indeed what happens. In Fig. 1(b), the green color indicates the validity island in the parameter space of (γ,H), where our theory agrees with the experimental result of Ref. [20].

As we discussed earlier, the problematic part of data fitting in the weakly interacting picture is the medium doping regime $x \sim 0.1$, where the transition between the WAL and WL is smooth. Does our theory fit the data in such a region? The answer is given in Fig. 2, where we took the data for $x = 0.1$. Here again our theory is valid only in an island of parameter space (H,T). There are only four adjustable parameters: γ, β, q_χ, v_F. Others (T,H,μ) are plot variables. From the data fitting point of view, the 1.9 K data are difficult to fit because they have too steep a curvature near the zero magnetic field $H = 0$. If we fit them for a small field region, the medium and large field regions do not fit at all. We believe that at $T = 1.9$ K the Fermi surface is still not small enough and our theory cannot fit such a weakly interacting regime by tuning all four parameters.

Another important question is whether our result is universal, namely, independent of the details of the matter. To answer this question at least partially, we worked out two materials in the validity islands, which is shown in Fig. 3(b). Figure 3(a) shows a remarkable similarity in MC curves for different TI materials. The transition behavior seems be universal and well described by our theory.

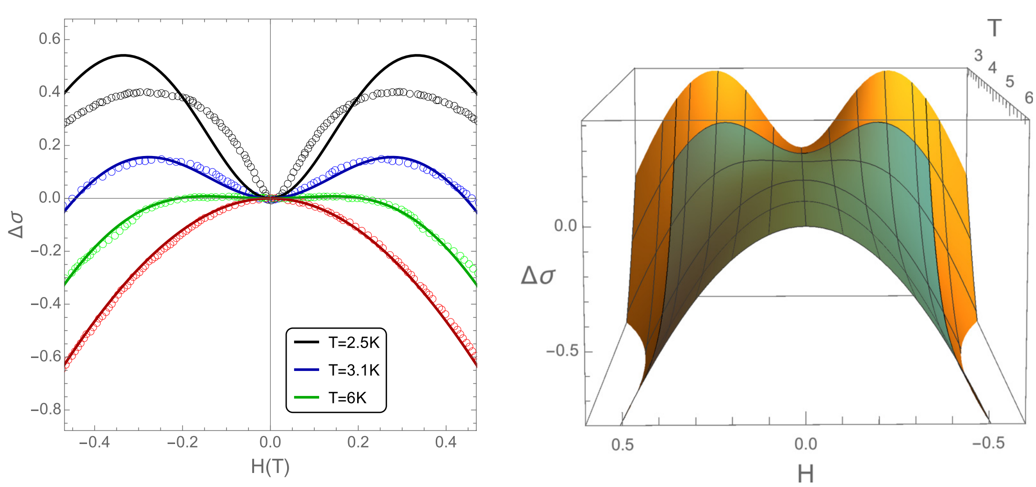

(a) (b)

FIG. 2. (a) Theory vs data (circle) for $x = 0.1$. $T = 1.9$ K is in the Fermi liquid regime where our theory does not work. (b) $\Delta\sigma$ as a function of H and T. Our theory works in the green colored island of (H,T) space, where the system is strongly correlated. We used $\beta^2 = \frac{2747}{(\mu\text{m})^2}$, $v_F = 7.5 \times 10^4$ m/s, $q_\chi = 7.12$.

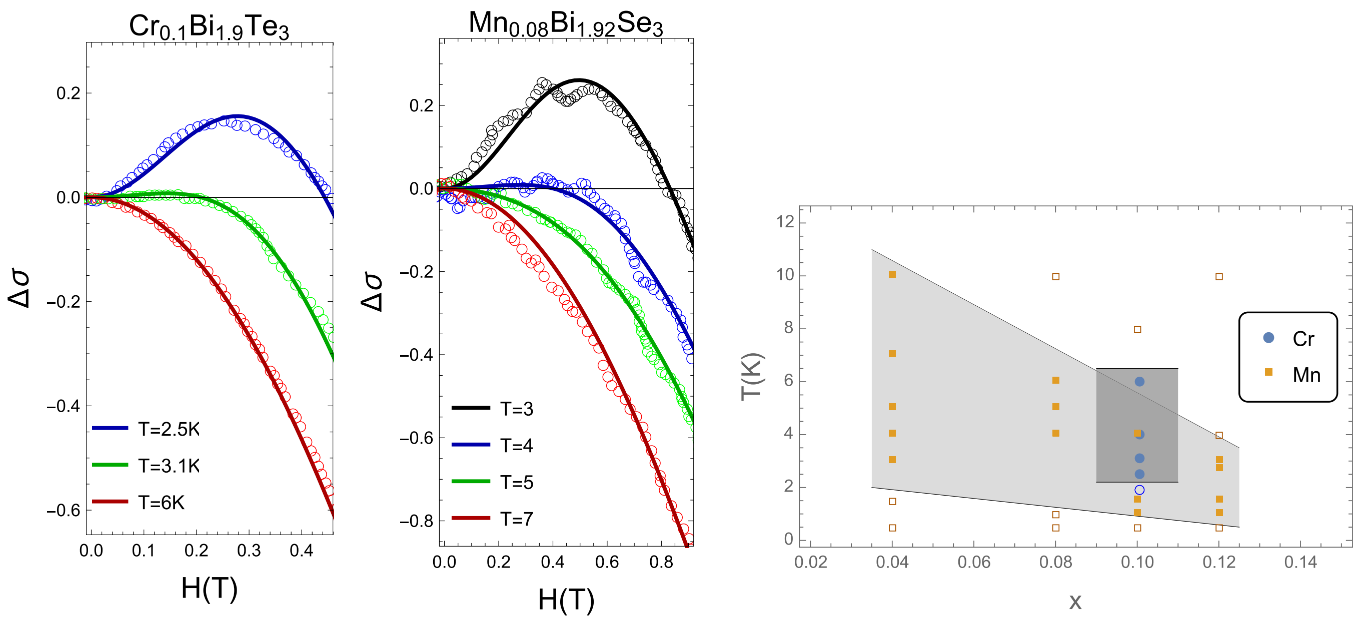

(a) (b)

FIG. 3. Universality of transition behavior: Two different materials are described by the same analytic expression with different parameter values. (a) MC for Cr-doped Bi_2Te_3 (left) and for Mn-doped Bi_2Se_3 (right). The data are from Refs. [19,20], respectively. (b) Strong correlation islands for the two. Bi_2Se_3 has the bigger island due to the bigger bulk gap.

In the weakly interacting picture, the nontrivial behavior of magnetoconductivity in the crossover regime is understood by the competition between antilocalization induced by spin-orbit coupling and localization by the surface gap. In the holographic picture, the enhancement in conductivity can be understood as the magnetoelectric effect or Witten effect. The interaction term dictates that an external magnetic field generates extra charge carriers $\delta q \sim \theta H$ to increase the conductivity. The result of the competition is a sign change in the curvature of the MC curve near $H = 0$, where

$$\Delta\sigma \sim -\frac{2(1-4\theta^2/9)}{r_0^2\beta^2}H^2 + O(H^4), \tag{14}$$

and $\theta = q_\chi\gamma\beta^2/r_0^2$. It also explains why the crossover from WAL to WL appears only in a relatively low but not a very low temperature region, because $r_0 \sim T$ for high temperatures and θ becomes small so that $1 - 2\theta/3$ cannot change the sign. This can be more precisely stated in terms of the phase diagram which is drawn in Fig. 2(b). Notice that there are only two phases. If $\gamma q_\chi > 1/4$, there is always a phase transition from WAL to WL.

Predictions. Finally, we give a list of predictions coming from our theory that can be testable by experiments.

(1) Near the Dirac point of small doping, we will find a transport anomaly, a large violation of the Wiedemann-Franz law just as for graphene.

(2) For undoped or weakly doped TIs, where one normally sees a sharp peak, the characteristic is of weak antilocalization. We predict that if one looks at the near Dirac point by adjusting the Fermi surface by gating, for example, one will see the disappearance of the sharp peak as we move down the Fermi surface.

(3) We claim that the transition behavior from WAL → WL in medium doping is universal: Namely, the magnetic conductivity of all two-dimensional Dirac materials with broken TRS can be described by our formula, independent of the details of the system. Here, we gave only two examples: Mn-doped Bi_2Se_3 in Fig. 2(a).

(4) For $Cr_xBi_{2-x}Te_3$ with $x = 0.1$, where the system in our picture is strongly interacting for $T \geqslant 2$ K, we expect that angle-resolved photoemission spectroscopy (ARPES) data will show a fuzzy density of states (DOS). This means that DOS will be nonzero in the region between dispersion curves, where the quasiparticle case would show empty DOS leading to the gap.

(5) All magnetotransport coefficients other than magnetoconductivity are predictions: That is, we calculated all the transport coefficients: Heat transports thermoelectric power, as well as magnetoconductance. Once we determine all the coefficients using MC data, all other transport results are predictions. It is a prediction for several observables as functions of multivariables (B,T,γ), containing a huge set of data.

Future directions. In this Rapid Communication, we examined the zero charge sector only. The nonzero charge parameter q will be discussed in a future publication. Other transport coefficients such as thermal conductivities and Seeback coefficients with or without magnetic fields are also important aspects that require further investigation. Graphene has an even number of Dirac cones, weak spin-orbit interactions, and different mechanisms for WL/WAL. Because of such differences, we need to find other interaction terms in the holographic model for graphene. It is also interesting to classify all possible patterns of interaction that provide the fermion surface gap in the presence of strong e−e correlations in our context.

Acknowledgments. We thank P. Kim for comments on the draft and for stimulating discussions on Dirac fluids. This work is supported by the Mid-career Researcher Program through the National Research Foundation of Korea Grant No. NRF-2016R1A2B3007687. Y.S. is also supported in part by the Basic Science Research Program through NRF Grant No. NRF-2016R1D1A1B03931443.

[1] S. Sachdev, *Quantum Phase Transitions,* 2nd ed. (Cambridge University Press, Cambridge, U.K., 2011).
[2] J. Zaanen, Y. Liu, Y.-W. Sun, and K. Schalm, *Holographic Duality in Condensed Matter Physics* (Cambridge University Press, Cambridge, U.K., 2015).
[3] E. Oh and S.-J. Sin, Phys. Lett. B **726**, 456 (2013).
[4] S.-J. Sin, J. Korean Phys. Soc. **66**, 151 (2015).
[5] S. A. Hartnoll, P. K. Kovtun, M. Müller, and S. Sachdev, Phys. Rev. B **76**, 144502 (2007).
[6] A. Lucas, J. Crossno, K. C. Fong, P. Kim, and S. Sachdev, Phys. Rev. B **93**, 075426 (2016).
[7] J. Maldacena, Int. J. Theor. Phys. **38**, 1113 (1999).
[8] E. Witten, Adv. Theor. Math. Phys. **2**, 253 (1998).
[9] S. S. Gubser, I. R. Klebanov, and A. M. Polyakov, Phys. Lett. B **428**, 105 (1998).
[10] J. Crossno, J. K. Shi, K. Wang, X. Liu, A. Harzheim, A. Lucas, S. Sachdev, P. Kim, T. Taniguchi, K. Watanabe, T. A. Ohki, and K. C. Fong, Science **351**, 1058 (2016).
[11] Y. Seo, G. Song, P. Kim, S. Sachdev, and S.-J. Sin, Phys. Rev. Lett. **118**, 036601 (2017).
[12] M. Z. Hasan and C. L. Kane, Rev. Mod. Phys. **82**, 3045 (2010).
[13] X.-L. Qi and S.-C. Zhang, Rev. Mod. Phys. **83**, 1057 (2011).
[14] R. Yu, W. Zhang, H.-J. Zhang, S.-C. Zhang, X. Dai, and Z. Fang, Science **329**, 61 (2010).
[15] L. Fu and C. L. Kane, Phys. Rev. Lett. **102**, 216403 (2009).
[16] X.-L. Qi, T. L. Hughes, and S.-C. Zhang, Phys. Rev. B **78**, 195424 (2008).
[17] G. Bergmann, Solid State Commun. **42**, 815 (1982).
[18] M. Liu, J. Zhang, C.-Z. Chang, Z. Zhang, X. Feng, K. Li, K. He, L.-l. Wang, X. Chen, X. Dai *et al.*, Phys. Rev. Lett. **108**, 036805 (2012).
[19] D. Zhang, A. Richardella, D. W. Rench, S.-Y. Xu, A. Kandala, T. C. Flanagan, H. Beidenkopf, A. L. Yeats, B. B. Buckley, P. V. Klimov, D. D. Awschalom, A. Yazdani, P. Schiffer, M. Z. Hasan, and N. Samarth, Phys. Rev. B **86**, 205127 (2012).
[20] L. Bao, W. Wang, N. Meyer, Y. Liu, C. Zhang, K. Wang, P. Ai, and F. Xiu, Sci. Rep. **3**, 2391 (2013).
[21] S. Hikami, A. I. Larkin, and Y. Nagaoka, Prog. Theor. Phys. **63**, 707 (1980).
[22] H.-Z. Lu, J. Shi, and S.-Q. Shen, Phys. Rev. Lett. **107**, 076801 (2011).
[23] In Refs. [18,32], the authors assigned weights for two HLN functions of opposite sign by hand to fit the data. In the graphene case, such transitions are better understood [33,34] in terms of intervalley scattering versus spin-orbit interactions.
[24] Y. Seo, K.-Y. Kim, K. K. Kim, and S.-J. Sin, Phys. Lett. B **759**, 104 (2016).
[25] N. Nagaosa, J. Sinova, S. Onoda, A. MacDonald, and N. Ong, Rev. Mod. Phys. **82**, 1539 (2010).
[26] A. M. Essin, J. E. Moore, and D. Vanderbilt, Phys. Rev. Lett. **102**, 146805 (2009).
[27] A. Donos and J. P. Gauntlett, J. High Energy Phys. 11 (2014) 081.
[28] T. Andrade and B. Withers, J. High Energy Phys. 05 (2014) 101.
[29] A. Amoretti and D. Musso, J. High Energy Phys. 09 (2015) 094.
[30] M. Blake, A. Donos, and N. Lohitsiri, J. High Energy Phys. 08 (2015) 124.
[31] K.-Y. Kim, K. K. Kim, Y. Seo, and S.-J. Sin, J. High Energy Phys. 07 (2015) 027.
[32] M. Lang, L. He, X. Kou, P. Upadhyaya, Y. Fan, H. Chu, Y. Jiang, J. H. Bardarson, W. Jiang, E. S. Choi *et al.*, Nano Lett. **13**, 48 (2012).
[33] E. McCann, K. Kechedzhi, V. I. Fal'ko, H. Suzuura, T. Ando, and B. L. Altshuler, Phys. Rev. Lett. **97**, 146805 (2006).
[34] F. V. Tikhonenko, A. A. Kozikov, A. K. Savchenko, and R. V. Gorbachev, Phys. Rev. Lett. **103**, 226801 (2009).